Department of Pharmacology[1], University of Zhejiang Chinese Medical, Hangzhou; School of Basic Medical Sciences and Forensic Medicine[2], Hangzhou Medical College, Hangzhou, China; Department of Pharmacology[3], School of Medicine Hallym University, Daegu, Korea

Acori tatarinowii rhizoma extract ameliorates Alzheimer's pathological syndromes by repairing myelin injury and lowering Tau phosphorylation in mice

Yunbo Fu[1,#], Yuanxiao Yang[2,#], Jianhong Shi[1], Kausik Bishayee[1], Luning Lin[1], Yiyou Lin[1], Yehui Zhang[1], Liting Ji[1,*], Changyu Li[1,*]

Received April 25, 2020, accepted May 30, 2020

**Corresponding authors: Liting Ji and Changyu Li, Department of Chinese Pharmacy, School of Science, Zhejiang Chinese Medical University, 548 Binwen Road, Hangzhou, Zhejiang, China*
lcyzcmu@sina.com (C.Y. Li), jenny8825@hotmail.com (L.T. Ji).
[#]Yunbo Fu and Yuanxiao Yang contributed equally to this work.

Pharmazie 75: 395-400 (2020) *doi: 10.1691/ph.2020.0492*

It has been shown that *Acori tatarinowii* rhizoma (ATR) extract can improve cognitive functions in Alzheimer Diseas (AD) patients or animal models. In this study, we have examined the activity of ATR in 3×Tg-AD model mice with different comprehensive behavioral tests like the Morris water maze and Y-maze test assay for behavior. Moreover, we performed LFB staining for myelin determination in the AD model mouse. By analyzing different pathways, we determined key proteins that are beneficial for ameliorating AD syndrome in the mouse. Periluminally, ATR treatment improved the learning and memory ability that was determined by comprehensive behavioral tests. Moreover, treatment reduces the p-Tau accumulation in the 3×Tg-AD mouse and the level of p-Tau accumulation was at per with the wildtype control mouse and improves the myelin lining in 3×Tg-AD mouse. In conclusion, our results indicate that ATR-treatment can improve the learning ability of AD model mice and the hyperphosphorylation of Tau protein was decreased. ATR can protect myelin lining from damage in AD syndrome.

1. Introduction

Alzheimer's disease (AD) is an age-related neurodegenerative disorder related to memory loss, cognitive dysfunction, and social disorders. The pathological characteristics of AD are formation and accumulation of extracellular amyloid-beta (Aβ) plaques, neurofibrillary tangles (NFTs) and that relate to neuronal cell death (Lane et al. 2018; Serrano-Pozo et al. 2011). There are about 50 million people with AD pathogenesis worldwide (Association 2016). Presently, two mainstream treatment strategies are available for AD, namely, acetylcholinesterase inhibitors, like donepezil, rivastigmine, and galantamine for patients with moderate AD pathogenesis; and the NMDA receptor blocker memantine for treating moderate to severe AD patients (Richardson et al. 2013; Tariot et al. 2004). However, the potential of these medicines is limited to inhibit the disease progression (Colovic et al. 2013). Previously, AD pathogenesis was generally considered as a disease of the gray matter (Nasrabady et al. 2018), but different observations from neuroimaging systems have shown white matter degeneration, demyelination and the inability of the oligodendrocytes to repair myelin damages (Nasrabady et al. 2018). Therefore, now myelin degradation is considered as another core feature of AD pathogenesis (Bartzokis 2011; Fern and Matute 2019; Matute 2010). In this study, we examined the ameliorating effect of the traditional Chinese medicine-*Acori tatarinowii* rhizoma (ATR) extract on AD pathogenesis and myelin protection and improvement in memory behavior.

According to traditional Chinese medicine, kidney essence shortage, marrow deficiency, and blood stagnation are major pathogenetic mechanisms in AD (Wang et al. 2011). ATR, the rhizome of *Acorus tatarinowii* schott, is long been a principal medicine in traditional Chinese formulas for the treatment of brain disorders, such as senile dementia, stroke aphasia, and amnesia (Mao et al. 2015). O55et (Zhang et al. 2007). However, specific mechanisms underlying the cognition-enhancing effects of ATR in AD model mouse have not been examined.

To explore the mechanism of action of ATR on AD, a triple-transgenic mouse model for AD (3×Tg-AD) was used. These mice, widely used for determining AD pathogenesis, are containing three mutations associated with AD and are viable, fertile, and display no initial gross physical or behavioral abnormalities. The translation of the overexpressed transgenes appearance is restricted to the central nervous system, hippocampus and cerebral cortex (Desai et al. 2009). We examined different behavioral and molecular or cellular parameters related to AD-like the "learning and memory ability" and p-Tau accumulation. The administration of ATR on 3×Tg-AD was able to cut down the AD-related symptomas. Moreover, myelin injury of 3×Tg-AD mouse improved under ATR treatment. Overall, ATR was found to be beneficial on 3×Tg-AD mice.

2. Investigations and results

2.1. GC-MS fingerprinting of ATR

The ATR extract contained different active ingredients. To understand the presence of beneficial active compounds like α-asarone and β-asarone, we analyzed ATR's chromatographic fingerprint by GC-MS, and compared with α-asarone and β-asarone as standards (Fig. 1). All GC-MS data, including retention characteristics, peak intensities, and integrated mass spectra of each sample were used for the qualitative analyses. A representative total ion chromatogram (TIC) of ATR is shown in Fig. 1A. The results of GC-MS showed that ATR exhibited characteristic peaks of α-asarone and β-asarone at 26.042 min and 28.166 min, respectively.

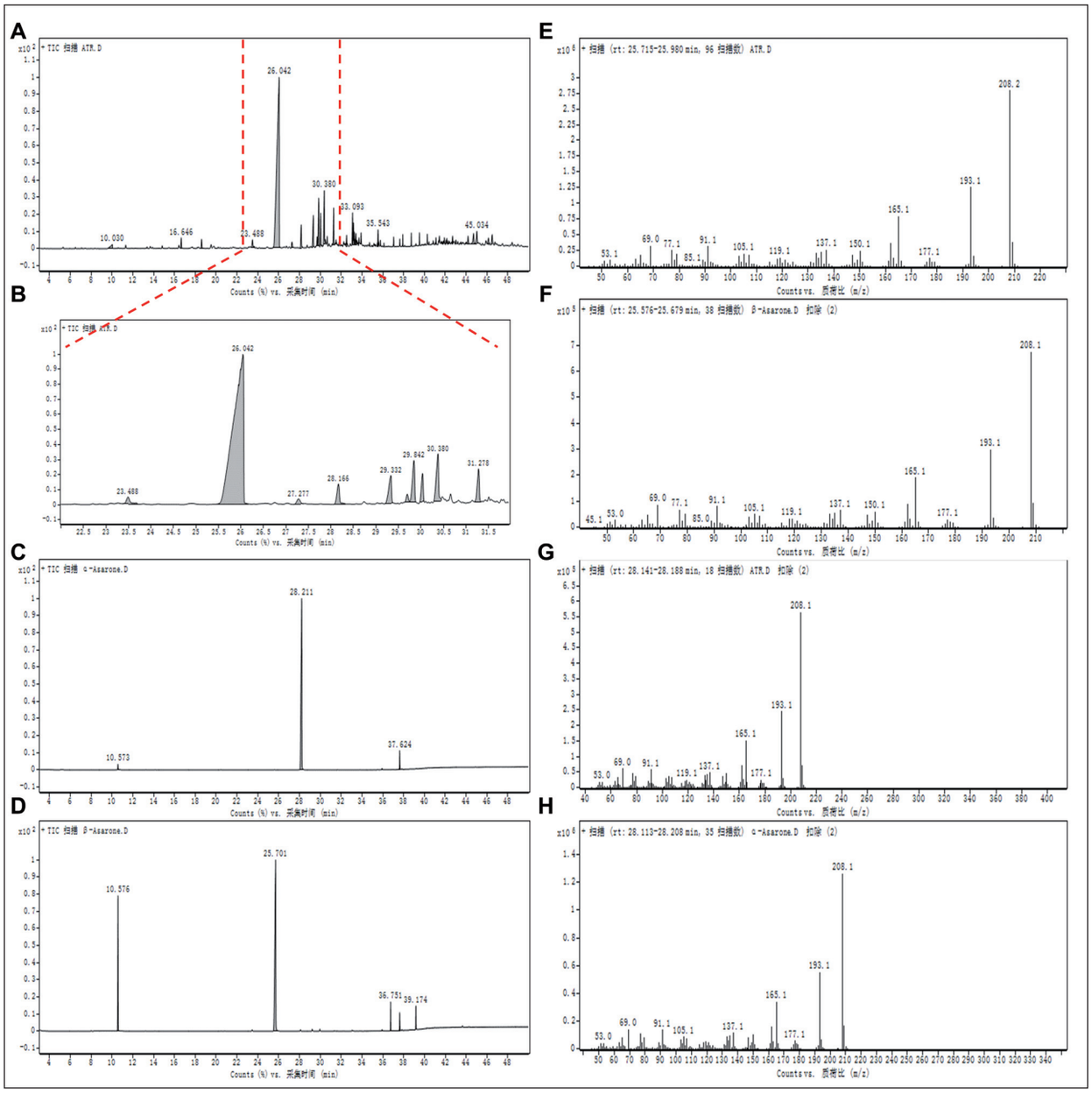

Fig. 1: The GC-MS fingerprint of ATR. (A-B) Signature for total ion chromatogram (TIC) of ATR at 4-48 min (A); and at 22.5-31.5 min (B); (C) TIC signature of α-asarone at 4-48 min; (D) TIC signature of β-asarone at 4-48 min; (E) MS signature of ATR at 2.715-2.980 min; (F) MS signature of β-asarone at 25.576-25.679 min; (G) MS signature of ATR at 28.141-28.188 min; (H) TIC signature of α-Asarone at 28.113-28.208 min.

2.2. ATR administration improves the learning and memory ability of 3×Tg-AD mice

ATR ameliorated different brain-related disorders (Lam et al. 2019; Yang et al. 2017). Keeping this in mind, we examined the potential of ATR against AD model mice. The 3×Tg-AD mouse administered with different doses of ATR was compared with the wild type non-AD mouse. To test memory and behavior, 3×Tg-AD of 9-month-old mice were used in the Morris water maze and Y-maze tests and compared with the non-AD wild type mouse of same age. Our results demonstrated that 9-month-old 3×Tg-AD mice showed memory problems and the group of ATR treated improved this condition, observed in the Morris water maze and Y-maze tests. After 5 days of the probe test, the escape latency time was significantly higher compared to the non-AD WT group (Fig. 2A). However, 3×Tg-AD mice treated with ATR 8 g/kg and ATR 16 g/kg showed a significant reduction in latency (Fig. 2B). Similarly, the place navigation tracking map, on the 5th day during the probe test, showed the track of 3×Tg-AD mice was messy, and a longer path was taken to find the platform compared to the non-AD WT group. ATR-treated 3×Tg-AD mice were able to find the platform path easier and more directional (Fig. 2A). Similarly, the number of platform crossings of Y-maze was significantly reduced in the 3×Tg-AD mice group compared to the WT mice group; however, significant reversal effects were observed in ATR-treated 3×Tg-AD mice with an increased number of platform crossings that suggest an improved memory performance (Fig. 2C). The percentage of residence time during the spatial probe test in the target quadrant showed the same results with platform crossings. In the Y-maze test, error rate (%) and number (n) were significantly higher in the 3×Tg-AD group but were significantly regulated in the ATR-treated 3×Tg-AD group (Fig. 2E-F). The results obtained by Y-maze and Morris water maze tests were consistent. Thus, all the data demonstrated that spatial memory impairment occurred in 3×Tg-AD mice, and ATR-treated mice showed an improved learning and memory ability of 3×Tg-AD mice.

2.3. ATR administration dismisses pathological syndromes in the 3×Tg-AD mice brain

The accumulation of phosphorylated Tau protein (p-Tau) in neurons is a major hallmark for AD (Duan et al. 2012). We observed the changes in the p-Tau accumulation in 3×Tg-AD mice. While comparing with the non-AD mouse, the accumulation of p-Tau was increased in 3×Tg-AD mice (Fig. 3A-B). We stained the hippocampus region of the mouse brain to investigate we examined the recovery of neurons with myelin in 3×Tg-AD mice brain by ATR administration. We performed LFB staining on corpus callosum of non-AD, 3×Tg-AD mice and on 3×Tg-AD mice treated with different doses of ATR. As a result, we found that ATR administration ameliorated the damages of myelin in 3×Tg-AD mice while comparing with non-AD mice (Fig. 4). This result might suggest that the anti-inflammatory properties of ATR extract effectively repaired the myelin injury of 3×Tg-AD mice.

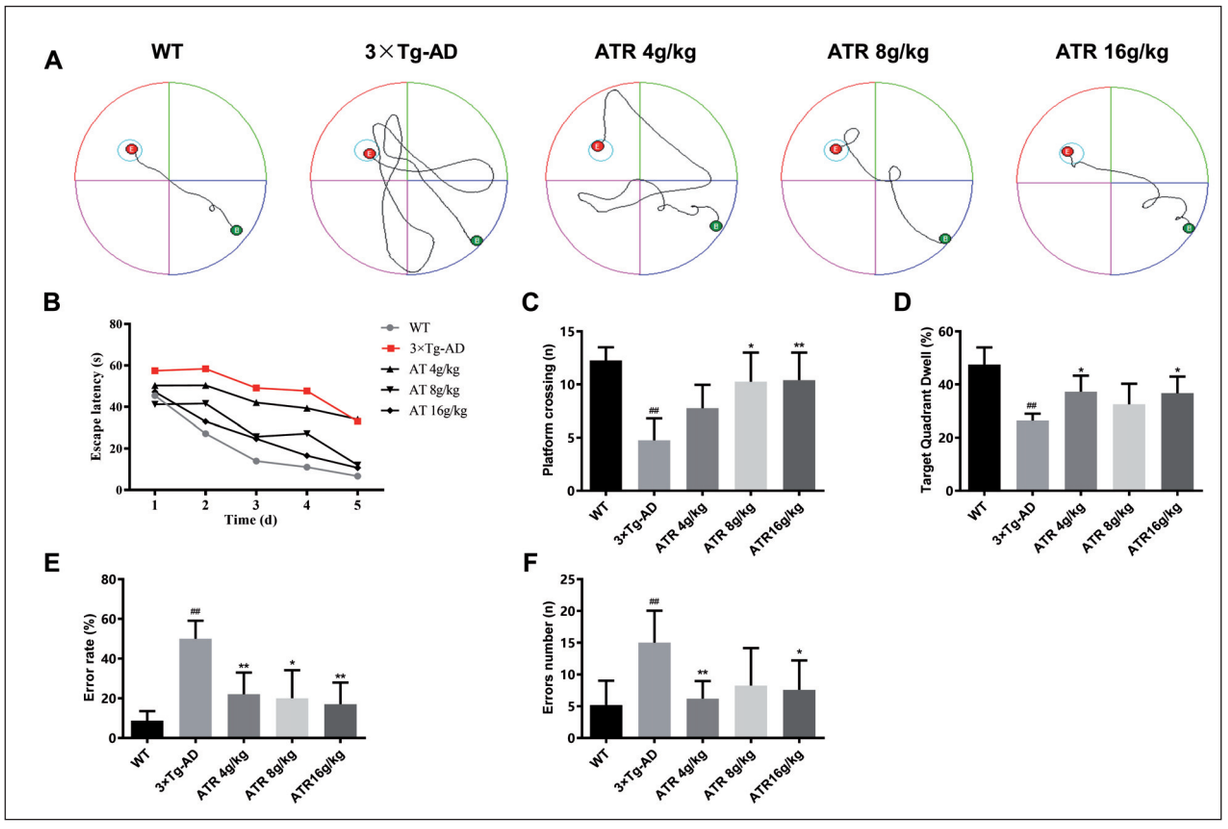

Fig. 2: Learning and memory ability assessed by the Morris water maze and Y-maze test. (A) Navigation tracking in day5. (B) The escape latency during training days. (C) Platform crossings on the test day. (D) The percentage of time spent in this quadrant. (E) Number of false reactions in all reactions. (F) Rate of false reactions in all reactions. [WT, wild-type mice; 3×Tg-AD, triple transgenic Alzheimer's disease model; ATR: 3×Tg-AD mice treated with ATR. Data are presented as mean ± SD (n = 6 in each group). One-way ANOVA followed by post-hoc analysis. ## $p < 0.01$ versus and # $p < 0.05$ versus the WT group; ** $p < 0.01$ and * $p < 0.05$ versus the 3×Tg-AD group.]

the potency of ATR on 3×Tg-AD mice. We applied different doses of the extract for three months' tenure and then checked the p-Tau accumulation in the hippocampus. We found that p-Tau expression was significantly diminished in ATR treated mice (Fig. 3A-B). Furthermore, we compared the p-Tau versus Tau expression by Western blot in non-AD, 3×Tg-AD mice and ATR (ATR 16 g/kg) treated-3×Tg-AD mice. We found that the ratio between p-Tau and Tau was significantly increased in 3×Tg-AD mice brain and was significantly decreased while treated with ATR extract (Fig. 3C-D). Tau protein was extensively phosphorylated in the 3×Tg-AD mice brain and the phosphorylation was reduced by ATR-administration without changing the total Tau protein expression while comparing with non-AD mice.

2.4. ATR administration repairs the myelin injury in 3×Tg-AD Mice

The disruption of myelin was observed in AD syndrome due to the inflammatory reactions (Zhan et al. 2015). Myelin is the fatty sheath of the neurons, which helps in the transmitting of neuron impulse (Stassart et al. 2018). In AD pathogenesis the loss of myelin sheath is a classic morphological sign (Bouhrara et al. 2018). In our study,

3. Discussion

AD pathogenesis alters the stability of neurons, due to the accumulation of different toxic substances like p-Tau. Moreover, neurons lose myelin that helps the neurons in transmitting signals. Among various treatment strategies for AD, Traditional Chinese Medicine offers promising remedies due to their non-toxic nature and their a long history in clinical applications (Tian et al. 2010). ATR is commonly used for treatment of AD and was shown to improve the cognitive ability in AD (Geng et al. 2010). In our study we showed different beneficial characters of ATR in a 3×Tg-AD mice model system.

In accordance with our findings, seventy-four volatiles were identified in ATR, among them, eleven of which were key bioactive principle components (Liu et al. 2017). Findings determined that 80% of those active compounds were volatile oil components and asarones like α-asarones and β-asarone. Compounds like α-asarones and β-asarone had previous histories in promoting neuronal differentiation and neurogenesis (Lam et al. 2016; Mao et al. 2015). According to previous findings, ATR could be beneficial for hindering neuro-degenerative disorders, and we demonstrated here that ATR administration ameliorated AD pathogenesis in mice.

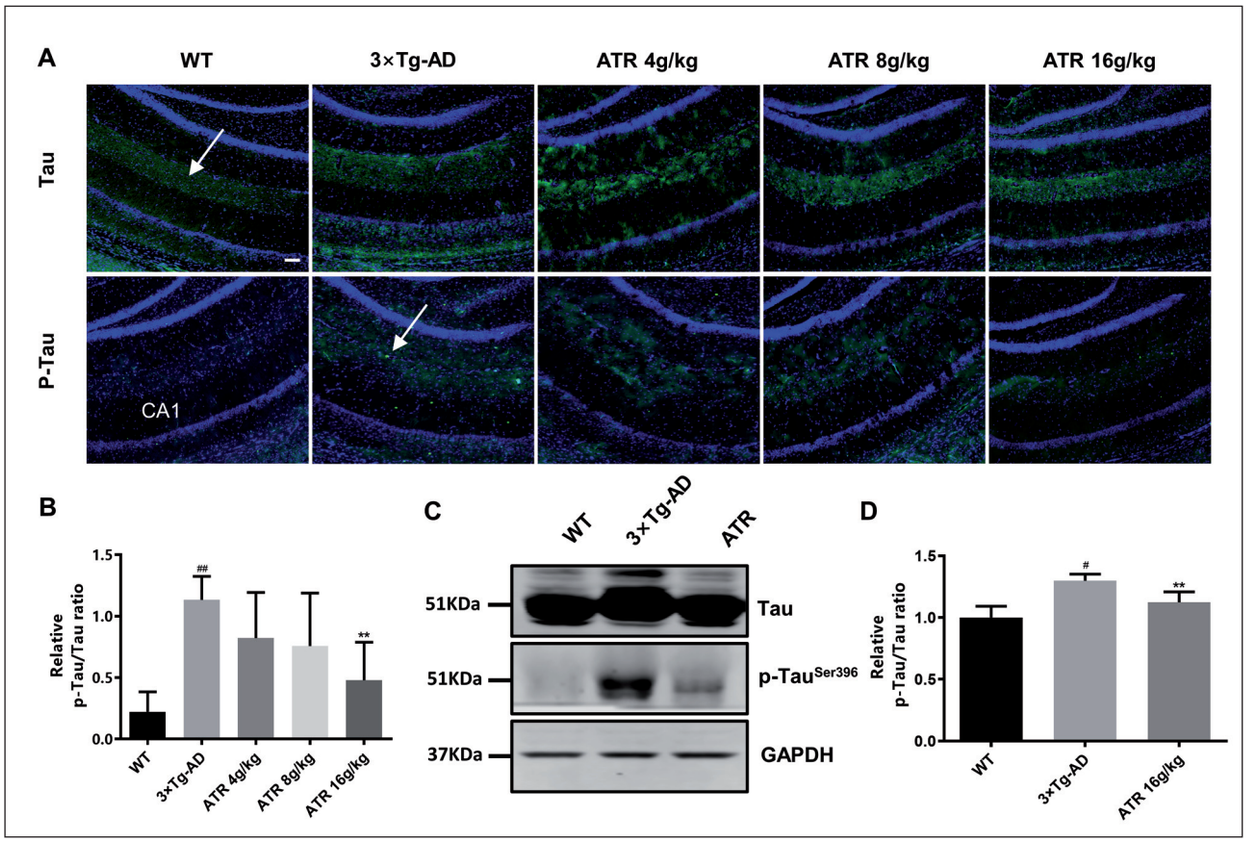

Fig. 3: ATR inhibited AD pathological changes in the hippocampus. (A-B) Tau and P-Tau expressions were evaluated by immunostaining using anti-Tau and anti-p-Tau antibodies, alexa fluro 488 conjugated secondary antibodies were used for detection in the different experimental groups, Scale bar = 100 μm. The expression was quantified and plotted as histogram in (B). (C) Western blot analysis of the Tau, and p-Tau (ser396) expressions in brain hippocampus. (D) Ration of p-Tau/Tau and normalized to GAPDH. The images were quantified using ImageJ software. [WT, wild-type mice; 3×Tg-AD, triple transgenic Alzheimer's disease model; ATR: 3×Tg-AD mice treated with ATR. Data were presented as mean±SD (n = 3 in each group). One-way ANOVA followed by post-hoc analysis. ## $p < 0.01$ versus the WT group; ** $p < 0.01$ and * $p < 0.05$ versus the 3×Tg-AD group.]

The current trends in AD treatment focus on prevention or early intervention (Crous-Bou et al. 2017; Yiannopoulou and Papageorgiou 2013). Studies have shown that 3×Tg-AD mice begin to develop Aβ plaques in the tail hippocampus at six months of age (Belfiore et al. 2019). In our study, we used five months old 3×Tg-AD mice for treatment. Through different experimental setup, we found that ATR administration improved cognitive functions in 3×Tg-AD mice, and had inhibitory effects on AD pathology. These data were consistent with previous reports on ATR and its formulated decoction to improve cognitive dysfunction in AD mouse model (Hou et al. 2014; Lam et al. 2017). More studies reported that the compounds like β-asarone (Deng et al. 2016) and Jowiseung-chungtang (Shin et al. 2018) have the properties like anti-Aβ aggregation and resveratrol (Sun et al. 2019) reducing the phosphorylation of Tau. We found that the Tau protein was extensively phosphorylated in the 3×Tg-AD mice brain and the phosphorylation was reduced by ATR-administration without changing the total Tau protein expression while comparing with non-AD control mice.

Degradation of the myelin sheath is closely related to AD pathogenesis (Cai and Xiao 2016; Dadar et al. 2019). Myelin helps in transmitting the neuronal signals at axon connections in the brain network (Nave and Werner 2014; Timmler and Simons 2019). Loss of myelin integrity in a neuronal circuit can lead to cognitive decline in AD (Fornito et al. 2015; Pievani et al. 2014). We found that the corpus callosum in 3×Tg-AD mice displayed loss in neurofibrillary myelin. However, the mechanism behind this repair process is unknown. Combining these findings, the ATR administration on 3×Tg-AD mice alleviated myelin lesions, which may be one of the important reasons for delaying the development of the disease.

In conclusion, we demonstrated that ATR administration was improved the learning and memory ability of 3×Tg-AD mice and decreased the phosphorylation of Tau protein, and promoted repair of myelin damage. Our findings endorsed a new mechanism for the treatment of AD by ATR.

4. Experimental

4.1. Preparation of ATR decoction

Acori tatarinowii rhizoma (purchased from the pharmaceutical factory of Zhejiang Traditional Chinese University, Lot.180601) was placed in a medicine pot, filled up with cold distilled water equivalent to ten-time volume of the ingredients, and soaked for two hours, then boiled for thirty minutes and filtered. The distilled water equivalent to ten-time volume of the extract was added and continued boiling for more twenty minutes and then filtered again. The fluids were concentrated on a water bath until 1 mL decoction containing 1.6 g crude drug and dilute it with double distilled water to 0.8g/ml and 0.4g/ml.

4.2. Animals and ATR administration

All animals were males and five months old. Twenty-five male 3×Tg-AD mice harboring APPSwe, tauP301L and PSEN1M146V transgenes and male wild-type mice (WT) (strain: B6) were randomly divided into wild type group, model group, ATR 4.0 g/kg group, ATR 8.0 g/kg group and ATR 16.0 g/kg group. The mice in each group received intragastrically 1 ml extract/100 g of body weight. The drug concentration was 0.4 g/ml for ATR 4 g/kg group, 0.8 g/ml for ATR 8 g/kg group, 1.6 g/ml for ATR 16 g/kg group, WT and 3×Tg-AD group were given the same volume of saline, once a day, for 4 months. All the animals were housed at 22±2 °C with 50-60% relative humidity. A 12 h light/12 h dark cycle was set, and the animals had free access to standard diet and water. All animal experiments were performed in accordance with NIH laboratory animal care and use guidelines (https://www.ncbinlm.nih.gov/books/NBK54050) under the supervision of the laboratory animal management and ethics committee of Zhejiang Traditional Chinese Medicine University (project code: ZSLL-2018- 17).

4.3. Specimen preparation

After 120 days of incubation, the mice were subjected to cardiac perfusion at the set time point: The mice were anesthetized with 0.3% sodium pentobarbital and the

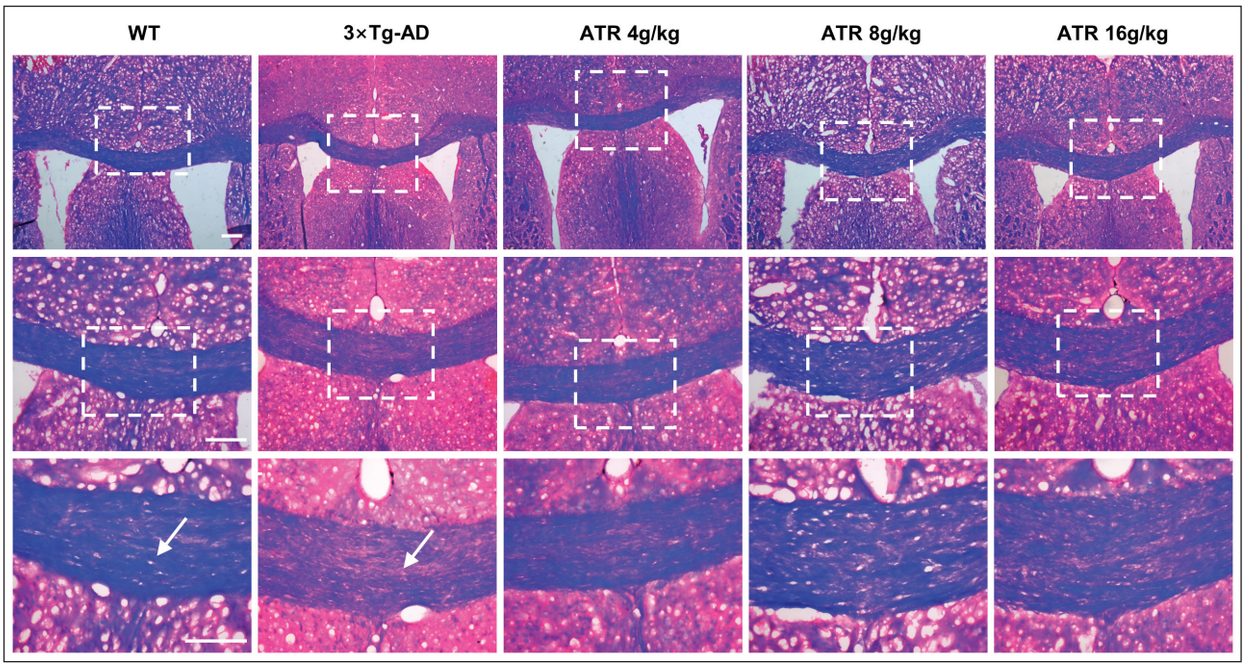

Fig. 4: The LFB staining results of myelin in different groups of mice, scale bar = 100 μm. WT, wild-type mice; 3×Tg-AD, triple transgenic Alzheimer's disease model; ATR: 3×Tg-AD mice treated with ATR.

thoracic cavity was opened and an infusion needle was inserted into the left ventricle. A cut was made at the right atrial appendage, and first infused with 0.9% saline for 5 min, waited for the liver to turn into white color, then infused with 4% paraformaldehyde for 15 min, craniotomy was performed and the brain was removed and kept in the above perfusate in a refrigerator at 4 °C for overnight, then the brain was immersed to dehydrate in 20% sucrose solution, and then with 30 % sucrose solution. The brain was sliced to a thickness of 10 μm and stored the slices at -80 °C for use.

4.4. GC-MS analysis

GC-MS analyses were conducted using a gas chromatograph (Agilent 7890-5977A, United States) coupled with an Agilent 7890-5977A mass spectrometer. The initial temperature set up of the column was 60 °C for 1 min. The column temperature was raised in three parts, firstly, from 60 to 120 °C at a rate of 5 °C/min, then from 120 to 150 °C at a rate of 2 °C/min and, lastly, from 150 to 280 °C for 10 °C/min. 1.0 μL of the sample was injected into the fused-silica capillary column DV-5 (30 m×0.25 mm with i.d. film thickness of 0.25 μm) with a split ratio of 1:10. High-purity helium was used as an inert carrier gas and the flow rate for it was set at 1.0 ml/min. The injector temperature was set at 250 °C. The specific conditions for mass spectrometry was set as follows: interface temperature 250 °C; ion source temperature 200 °C; ionization voltage 70 eV; and full scan mode in the 45-500 m/z mass ranges with 1.0/s scan velocities.

4.5. Morris water maze experiment

A Morris water maze test system was used (Panlab Harvard Apparatus, 3.0) for this experiment. First, for 1 to 5 days of the Morris water maze experiment, the platform was kept 1 cm below the water surface. The mice of each group were placed in water from the four quadrants according to the grouping number. Each animal went for three trials. First, place the animal on the platform for fifteen seconds. Then we let the animal search for the platform for a maximum of sixty seconds. After the trial, the mice were learned to search for the platform and climb up. During the observation period, the time required to find the platform was recorded. On the sixth day of the water maze experiment, the platform was removed and the mice were placed sequentially from the four quadrants, recording the number of passes through the original platform position in one minute.

4.6. Y maze experiment

The mice were placed in the arm of the programmed labyrinth of the grid. The three arms of the labyrinth contained a light signal. After the lamp was on, the grid that was lit for 5 s and was not energized, and the remaining 2 grids were energized to stimulate the mice to escape. The energized bright arms were reached for 15 s after reaching the bright arms, and the mice were trained in 3 arms for 3 days, and the test was performed on the fourth day.

4.7. LFB staining

Slices were placed in 0.1% LFB for 10 h, and in 95% alcohol, and in 0.05% Lithium carbonate for 10 s, after washed in distilled for a while, then the slices were kept in tar purple dye solution for 10 minutes, and then washed with distilled water. 70% of alcohol was used for the color saparation, and for conventional dehydration.

4.8. Immunofluorescence staining

The frozen sections were rewarmed for 15 min and fixed in 4% paraformaldehyde for 15 min. The sections were taken out and placed in a repair kit of antigen repair buffer for antigen retrieval in a microwave oven. The slides were washed with 0.1% PBST and blocked with 5% BSA for 60 min and then incubated with primary antibodies: rabbit anti-Tau (YT4546, 1:400, immunoway, United States), a rat anti-Tau of phospho Ser396 (YP0263, 1:400, immunoway, United States). Therafter the slides were washed four times with PBST for 5 min each. After the sections were slightly dried, the secondary antibody was added dropwise to the tissues and incubated at room temperature for 120 min in the dark. Slides were washed 4 times with 0.1% PBST for 5 min each and was observed under a microscope (Zeiss, AXIO SCOPE.A1, Germany).

4.9. Immunoblotting

For immunoblotting, 25 μg of proteins (control, 3×Tg-AD, and ATR 16 g/kg groups) were separated by 10% SDS-PAGE and blotted onto a nitrocellulose membrane (Bio-Rad, Hercules, CA, USA). Membranes were blocked with 5% bovine serum albumin in T-TBS for 90 min at room temperature and incubated individually overnight at 4 °C with primary anti-bodies: rabbit anti-Tau (YT4546, 1:5000, Immunoway, United States), rabbit anti-pSer396-Tau (YP0263, 1:1000, Immunoway, United States) and rabbit anti-GAPDH (ER1706-83, 1:1000, HuaAn, China). After three-time washing with T-TBS, the membranes were incubated for 1 h at room temperature with secondary antibody: anti-rabbit (RS23220, 1:5000, Cell Signaling, United States). The blots were then imaged and analyzed by software from Odyssey Imager (LI-COR, LI-COR Odyssey Clx, United States). Data quantification was done using ImageJ (NIH, United States).

4.10. Statistics

Statistical analyses were performed with SPSS 24.0 software. Data were expressed as mean±standard deviation (SD) and analyzed using the one-way analysis of variance (ANOVA) followed by Tukey's post hoc test for comparisons between three groups. $P<0.05$ was considered statistically significant.

Acknowledgments/conflicts of interest: This work was supported by the National Natural Science Foundation of China [81673839]; University of Zhejiang Chinese Medical [752213A00404; 751200F050]. All sources of funding for the research declare that they have no competing financial or personal interests.

References

Association (2016) 2016 Alzheimer's disease facts and figures. Alzheimers Dement 12: 459–509.

Bartzokis G (2011) Alzheimer's disease as homeostatic responses to age-related myelin breakdown. Neurobiol Aging 32: 1341–1371.

Belfiore R, Rodin A, Ferreira E, Velazquez R, Branca C, Caccamo A, Oddo S (2019) Temporal and regional progression of Alzheimer's disease-like pathology in 3xTg-AD mice. Aging Cell 18: e12873

Bouhrara M, Reiter DA, Bergeron CM, Zukley LM, Ferrucci L, Resnick SM, Spencer RG (2018) Evidence of demyelination in mild cognitive impairment and dementia using a direct and specific magnetic resonance imaging measure of myelin content. Alzheimers Dement 14: 998–1004.

Cai Z, Xiao M (2016) Oligodendrocytes and Alzheimer's disease. Int J Neurosci 126: 97–104.

Colovic MB, Krstic DZ, Lazarevic-Pasti TD, Bondzic AM, Vasic VM (2013) Acetylcholinesterase inhibitors: pharmacology and toxicology. Curr Neuropharmacol 11: 315–335.

Crous-Bou M, Minguillon C, Gramunt N, Molinuevo JL (2017) Alzheimer's disease prevention: from risk factors to early intervention. Alzheimers Res Ther 9: 71.

Dadar M, Maranzano J, Ducharme S, Collins DL (2019) White matter in different regions evolves differently during progression to dementia. Neurobiol Aging 76: 71–79.

Deng M, Huang L, Ning B, Wang N, Zhang Q, Zhu C, Fang Y (2016) beta-asarone improves learning and memory and reduces Acetyl Cholinesterase and Beta-amyloid 42 levels in APP/PS1 transgenic mice by regulating Beclin-1-dependent autophagy. Brain Res 1652: 188–194.

Desai MK, Sudol KL, Janelsins MC, Mastrangelo MA, Frazer ME, Bowers WJ (2009) Triple-transgenic Alzheimer's disease mice exhibit region-specific abnormalities in brain myelination patterns prior to appearance of amyloid and tau pathology. Glia 57: 54–65.

Duan Y, Dong S, Gu F, Hu Y, Zhao Z (2012) Advances in the pathogenesis of Alzheimer's disease: focusing on tau-mediated neurodegeneration. Translat Neurodegen 1: 24

Fern R, Matute C (2019) Glutamate receptors and white matter stroke. Neurosci Lett 694: 86–92.

Fornito A, Zalesky A, Breakspear M (2015) The connectomics of brain disorders. Nature Rev Neurosci 16: 159–172.

Geng Y, Li C, Liu J, Xing G, Zhou L, Dong M, Li X, Niu Y (2010) Beta-asarone improves cognitive function by suppressing neuronal apoptosis in the beta-amyloid hippocampus injection rats. Biol Pharm Bull 33: 836–843.

Hou Y, Wang Y, Zhao J, Li X, Cui J, Ding J, Wang Y, Zeng X, Ling Y, Shen X, Chen S, Huang C, Pei G (2014) Smart Soup, a traditional Chinese medicine formula, ameliorates amyloid pathology and related cognitive deficits. PloS one 9: e111215

Lam KY, Chen J, Lam CT, Wu Q, Yao P, Dong TT, Lin H, Tsim KW (2016) Asarone from Acori tatarinowii rhizoma potentiates the nerve growth factor-induced neuronal differentiation in cultured PC12 cells: a signaling mediated by protein kinase A. PloS one 11: e0163337,

Lam KYC, Wu QY, Hu WH, Yao P, Wang HY, Dong TTX, Tsim KWK (2019) Asarones from Acori tatarinowii Rhizoma stimulate expression and secretion of neurotrophic factors in cultured astrocytes. Neurosci Lett 707: 134308

Lam KYC, Yao P, Wang H, Duan R, Dong TTX, Tsim KWK (2017) Asarone from Acori tatarinowii rhizome prevents oxidative stress-induced cell injury in cultured astrocytes: A signaling triggered by Akt activation. PloS one 12: e0179077

Lane CA, Hardy J, Schott JM (2018) Alzheimer's disease. Eur J Neurol 25: 59–70.

Liu W, Zhang B, Xin Z, Ren D, Yi L (2017) GC-MS Fingerprinting combined with chemometric methods reveals key bioactive components in Acori tatarinowii rhizoma. Int J Mol Sci 18: 1342.

Mao J, Huang S, Liu S, Feng XL, Yu M, Liu J, Sun YE, Chen G, Yu Y, Zhao J, Pei G (2015) A herbal medicine for Alzheimer's disease and its active constituents promote neural progenitor proliferation. Aging Cell 14: 784–796.

Matute C (2010) Calcium dyshomeostasis in white matter pathology. Cell Calcium 47: 150–157.

Nasrabady SE, Rizvi B, Goldman JE, Brickman AM (2018) White matter changes in Alzheimer's disease: a focus on myelin and oligodendrocytes. Acta Neuropathol Comm 6: 22.

Nave KA, Werner HB (2014) Myelination of the nervous system: mechanisms and functions. Ann Rev Cell Develop Biol 30: 503–533.

Pievani M, Filippini N, van den Heuvel MP, Cappa SF, Frisoni GB (2014) Brain connectivity in neurodegenerative diseases--from phenotype to proteinopathy. Nature Rev Neurol 10: 620–633.

Richardson C, Gard PR, Klugman A, Isaac M, Tabet N (2013) Blood pro-inflammatory cytokines in Alzheimer's disease in relation to the use of acetylcholinesterase inhibitors. Int J Geriatr Psychiatry 28: 1312–1317.

Serrano-Pozo A, Frosch MP, Masliah E, Hyman BT (2011) Neuropathological alterations in Alzheimer disease. Cold Spring Harbor Perspect Med 1: a006189

Shin SJ, Jeong YO, Jeon SG, Kim S, Lee SK, Nam Y, Park YH, Kim D, Lee YS, Choi HS, Kim JI, Kim JJ, Moon M (2018) Jowiseungchungtang inhibits amyloid-beta aggregation and amyloid-beta-mediated pathology in 5XFAD mice. Int J Mol Sci 19: 4026.

Stassart RM, Mobius W, Nave KA, Edgar JM (2018) The axon-myelin unit in development and degenerative disease. Frontiers Neurosci 12: 467

Sun XY, Dong QX, Zhu J, Sun X, Zhang LF, Qiu M, Yu XL, Liu RT (2019) Resveratrol rescues tau-induced cognitive deficits and neuropathology in a mouse model of tauopathy. Curr Alzheimer Res 16: 710–722.

Tariot PN, Farlow MR, Grossberg GT, Graham SM, McDonald S, Gergel I (2004) Memantine treatment in patients with moderate to severe Alzheimer disease already receiving donepezil: a randomized controlled trial. JAMA 291: 317–324

Tian J, Shi J, Zhang X, Wang Y (2010) Herbal therapy: a new pathway for the treatment of Alzheimer's disease. Alzheimers Res Ther 2: 30.

Timmler S, Simons M (2019) Grey matter myelination. Glia 67: 2063–2070.

Wang YB, Guo L, Dou ZF, Wang YX (2011) Discussion on the etiology and pathogenesis of the Alzheimer's disease in Chinese medicine. Chin Arch Trad Chin Med 29: 743–745.

Yang Y, Xuan L, Chen H, Dai S, Ji L, Bao Y, Li C (2017) Neuroprotective effects and mechanism of beta-asarone against A beta1-42-induced injury in astrocytes. Evid Based Complement Alternat Med 2017: 8516518

Yiannopoulou KG, Papageorgiou SG (2013) Current and future treatments for Alzheimer's disease. Ther Adv Neurol Disord 6: 19–33.

Zhan X, Cox C, Ander BP, Liu D, Stamova B, Jin LW, Jickling GC, Sharp FR (2015) Inflammation combined with ischemia produces myelin injury and plaque-like aggregates of myelin, amyloid-beta and AbetaPP in adult rat brain. J Alzheimers Dis 46: 507–523.

Zhang H, Han T, Yu CH, Rahman K, Qin LP, Peng C (2007) Ameliorating effects of essential oil from Acori graminei rhizoma on learning and memory in aged rats and mice. J Pharm Pharmcol 59: 301–309.